A Simulated Annealing Global Maximum Power Point Tracking Approach for PV Modules Under Partial Shading Conditions

Sarah Lyden, *Student Member, IEEE*, and Md. Enamul Haque, *Senior Member, IEEE*

***Abstract*—This paper proposes a simulated annealing (SA)-based global maximum power point tracking (GMPPT) technique designed for photovoltaic (PV) systems which experience partial shading conditions (PSC). The proposed technique is compared with the common perturb and observe MPPT technique and the particle swarm optimization method for GMPPT. The performance is assessed by considering the time taken to converge and the number of sample cases where the technique converges to the GMPP. Simulation results indicate the improved performance of the SA-based GMPPT algorithm, with arbitrarily selected parameters, in tracking to the global maxima in a multiple module PV system which experiences PSC. Experimental validation of the technique is presented based on PV modules that experience nonuniform environmental conditions. Additionally, studies regarding the influence of the key parameters of the SA-based algorithm are described. Simulation and experimental results verify the effectiveness of the proposed GMPPT method.**

***Index Terms*—Maximum power point trackers, particle swarm optimization (PSO), photovoltaic (PV) systems, simulated annealing (SA).**

I. Introduction

MAXIMUM power point tracking (MPPT) is an important concern in the operation of photovoltaic (PV) systems. Each PV cell has a limited efficiency at converting the energy in sunlight into electricity. Additionally, the PV cell exhibits a nonlinear power–voltage (*P–V*) and current–voltage (*I–V*) characteristic, which means that there is a single optimal operating point which corresponds to the maximum power and maximum efficiency. This optimal operating point will vary as the environmental conditions change. When multiple cells are connected in series and parallel arrangements, the *I–V* and *P–V* characteristics become more complex and may exhibit multiple local maxima.

MPPT approaches are usually applied to try to maintain the system operation at the optimal operating point. Many MPPT methods have been proposed with the aim of achieving consistent operation at the MPP [1]–[6]. However, when the environmental conditions vary across the modules, conventional MPPT techniques are not often able to distinguish between global and local maxima resulting in the system potentially operating at a lower power level.

The environmental conditions that PV systems operate under, particularly in residential areas, rarely present uniform operating conditions. There are several objects including trees and other houses which may shade the modules throughout the day, cell mismatch can occur creating an internal shading type phenomena, and the passage of clouds over the system will cause varying irradiance levels [7], [8]. Under these conditions, conventional MPPT techniques will frequently track to a local MPP as they cannot distinguish between local and global maxima. While some techniques have been proposed to enable global MPPT (GMPPT) under such conditions, these frequently result in larger system implementation cost [9]–[13], have increased complexity [9], [10], [14], may not always guarantee GMPPT, or experience significant power losses in the tracking process [15]–[17]. In some cases, these GMPPT methods need to be optimized for each individual PV system or are strongly dependent on the starting value [18]–[20].

The perturb and observe (P&O) technique is frequently used in PV systems due to its low cost and simple implementation [17], [21]–[23]. P&O-based techniques are limited by a tradeoff between step size and tracking speed, exhibit poor performance under rapid changes in irradiance, and stop at the first maxima, regardless of if this is the GMPP [17], [21]–[24].

Particle swarm optimization (PSO) has been proposed as a GMPPT technique based on the behavior of fish schooling and birds flocking [19], [25]–[28]. In this technique, particles collectively solve a problem by sharing information to find the best solution. The technique is limited by the presence of random variables in its implementation, and it requires several parameters to be defined for each system [19].

The technique proposed in this paper is reliable at tracking to the GMPP, and does so with complexity similar to the standard implementation of the P&O technique. Technique performance is compared against the P&O and PSO methods to show that accurate GMPPT performance can be achieved with a minimal complexity implementation. The purpose of comparing the proposed method with P&O is because the methods have similar complexity, yet a considerable difference in performance when applied to a system under nonuniform environmental conditions. PSO is also used as a comparison technique, as it is a common technique designed specifically for partial shading conditions (PSC). The objectives of the proposed GMPPT method are to enable GMPPT in PV systems in a minimal complexity implementation and with limited dependence on system specific parameters.

Manuscript received February 2, 2015; revised April 23, 2015 and June 23, 2015; accepted July 29, 2015. Date of publication August 13, 2015; date of current version January 7, 2016. Recommended for publication by Associate Editor V. Agarwal.

S. Lyden is with the School of Engineering and ICT, University of Tasmania, Hobart, Tas. 7005, Australia (e-mail: Sarah.Lyden@utas.edu.au).

M. E. Haque is with the School of Engineering, Deakin University, Geelong, Vic. 3220, Australia (e-mail: enamul.haque@deakin.edu.au).

Color versions of one or more of the figures in this paper are available online at http://ieeexplore.ieee.org.

Digital Object Identifier 10.1109/TPEL.2015.2468592

The proposed technique is based on the optimization technique of simulated annealing (SA). SA was proposed in 1980s by Kirkpatrick *et al.* [29] and Černý [30] as a global minimization method based upon the physical process of annealing in metals. In metallurgy, annealing occurs when metals are heated up to a high temperature such that they become molten, and are then cooled according to a particular cooling schedule until a minimum energy state is found [31]. Since 1980s, the technique has been applied to a variety of optimization problems [32]–[44]. In [40], the SA method is applied to MPPT in a simple PV system experiencing uniform conditions. This paper presents a more robust implementation of the SA method for MPPT, specifically under PSC. Consideration is also given to optimization of the parameters of the SA method for GMPPT, which has not previously been presented in the literature to the best of the authors' knowledge.

As PSC represent a more realistic operating condition for PV systems in residential environments, the SA method is developed and experimentally implemented in this paper in the context of PSC. The PSC considered combines the effect of the shading from objects in the environment, module mismatch, and variations in irradiance across the modules.

In Sections II and III, the P&O and PSO methods are described. In Section IV, the proposed SA GMPPT technique is defined. Section V discusses the simulation model used in the analysis, and Section VI describes the simulation results. Section VII details the experimental implementation and validation of the performance of the SA algorithm. In Section VIII, the key parameters of the SA method are explored in more detail. Finally, conclusions are provided in Section IX.

II. P&O MPPT Method

The P&O MPPT method is commonly implemented due to its simplicity and low cost compared with other methods [17], [21]–[23]. It is based on applying a perturbation in the control variable (usually voltage, although could be current or duty cycle) [45] and observing the corresponding change in power. On this basis, the change in power measured with respect to a known change in voltage can indicate the next perturbation direction needed to track to the MPP. As the P&O technique is a gradient-based method, it seeks the operating point where $\frac{dP}{dV} = 0$. This condition will exists at any local and any global maxima, and results in the P&O technique simply tracking until it locates any maxima. Once a maxima is located, the method will continue to oscillate around this point and will not explore the remaining search space until a change in the environmental conditions allows the method to track to an alternative point. By decreasing the step size, it is possible to converge to the MPP more precisely, but this is at the expense of the tracking speed.

The tracking direction of the P&O technique is determined by

$$\begin{aligned} \frac{dP}{dV} &> 0, \qquad \text{left of MPP} \\ \frac{dP}{dV} &= 0, \qquad \text{at MPP} \\ \frac{dP}{dV} &< 0, \qquad \text{right of MPP.} \end{aligned} \tag{1}$$

III. PSO MPPT Method

PSO uses a group of particles to collectively solve a problem. Each particle's position is updated based on its own best position and the global best position enabling the particles to converge to a global solution. The particle position at the next step is given by (2), where x_i^k is the previous particle position, x_i^{k+1} is the new particle position, and Φ_i^{k+1} is the particle's new velocity

$$x_i^{k+1} = x_i^k + \Phi_i^{k+1}. \tag{2}$$

The particle's velocity is calculated based on the particle's previous velocity, the differences between the particle's current position and the previous best position, and the difference between the particle's current position and the global best position. The particle velocity is calculated using (3) where ω is the inertia weight, c_1, c_2 are the acceleration coefficients, $r_1, r_2 \in U(0,1)$ are the random numbers, $P_{\text{best},i}$ is the personal best position of particle i, and G_{best} is the best position of all particles in the population

$$\Phi_i^{k+1} = \omega\Phi_i^k + c_1 r_1 (P_{\text{best},i} - x_i^k) + c_2 r_2 (G_{\text{best}} - x_i^k). \tag{3}$$

IV. Proposed GMPPT Method Based on SA

SA works to find an optimal solution by following the process of annealing in metals. Traditionally, in cooling metals in a controlled manner, the minimum energy state is sought. In applying the SA method to find the GMPP for a PV system, it is necessary to seek the maximum energy (or power) condition. The technique needs to be able to track to the GMPP rather than a local MPP which makes good use of the global searching behavior of the SA algorithm.

The SA algorithm requires an initial temperature, final temperature, and cooling rate. At each temperature, the algorithm performs several perturbations in the operating point (voltage) and measures the corresponding energy (power). This measured energy is compared with the current reference energy. If the new operating point has greater energy, then it will be accepted as the new operating point. If the new operating point has less energy than the reference operating point, then it may still be accepted depending on the acceptance probability. The acceptance probability relates to both the energy difference and the current temperature of the search [46], and at higher temperature, small reductions in energy are likely to be accepted [47]. As the temperature reduces, the likelihood that solutions with lower energy will be accepted reduces. The acceptance probability is given in (4), where P_k is the power at the current voltage, P_i is the power at the previous best operating point, and T_k is the current temperature of the system

$$Pr = \exp\left[\frac{P_k - P_i}{T_k}\right]. \tag{4}$$

The SA algorithm requires a cooling schedule which may be either static or adaptive [40]. This paper uses the common geometric cooling schedule, as given in (5), where T_k is the temperature for step k, T_{k-1} is the temperature at step $k-1$, and α is some constant ($\alpha < 1$) [35], [47]

$$T_k = \alpha T_{k-1}. \tag{5}$$

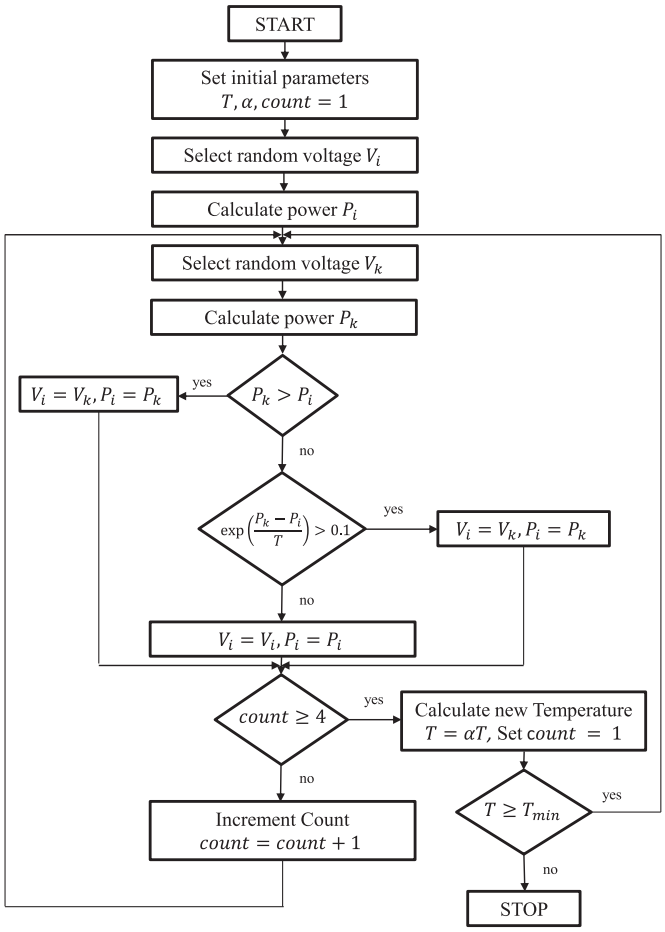

Fig. 1. Flowchart of the proposed SA GMPPT method.

As the temperature is updated every four random perturbations, the implementation represents inhomogeneous SA, as equilibrium is not required at each temperature level [46]. The SA algorithm implementations considered in this paper perform the following steps.

1) Set the initial parameters including the initial temperature, cooling rate α, neighbourhood size, and final temperature.
2) Select a random voltage V_i within the search range.
3) Calculate/measure the power P_i.
4) While the temperature is greater than the stopping criterion ($T_{\min}$), repeat the following:
   a) select a random voltage V_k;
   b) calculate/measure the power P_k;
   c) if the new power P_k is greater than the previous power P_i, the point V_k becomes the new operating point (i.e., $V_i = V_k$);
   d) otherwise, if the new power is less than the previous power, accept the operating point based on the acceptance probability given in (4);
   e) if four sample points have been considered at this temperature, reduce the temperature using the geometric cooling schedule given in (5).

The flowchart of the proposed GMPPT algorithm using the SA method is shown in Fig. 1.

V. Simulation Model and Technique Implementation

The eight-module case has been simulated using the single-diode model [48], [49] in MATLAB/Simulink. The *I–V* characteristic is given by

$$I = I_{\text{ph}} - I_0 \left[\exp\left(\frac{V + IR_s}{V_t}\right) - 1\right] - \frac{V + IR_s}{R_{\text{sh}}} \quad (6)$$

where I_{ph} is the light generated current, I_0 is the diode saturation current, R_s is the series resistance, and R_{sh} is the shunt resistance, and $V_t = \frac{kTAn_s}{q}$ is the junction thermal voltage (where k is the Boltzmann constant (1.38×10^{-23}J/K), A is the diode ideality factor, q is the electron charge (1.6×10^{-19} C), T is the temperature on absolute scale (K), and n_s is the number of series-connected cells in the module).

The simulation model is constructed on the basis of BP380 80-W PV modules [50]. The eight modules are connected in series and experience nonuniform environmental conditions due to a moving shadow caused by an obstacle in the environment. The obstacle has a length of 20 m, and a width of 0.5 m. It is positioned 10-m North and 5-m West of the eight-module PV system. The PV system is simulated to be located in Tasmania at the site of the Cape Grim weather monitoring site at latitude -40.6817, longitude 144.6892. At this site, 1-min solar irradiance data are recorded across the year.

The shading factor of each module is assessed by considering the number of cells in the module that may be shaded. A cell is considered to be shaded if its midpoint is within half of the shadow width from the central shadow projection. The shadow projection is evaluated by considering the geometry of the object and the location of the sun at the time of interest. The end point of the shadow is evaluated using the equations for the shadow geometry, and the central shadow projection is considered to be a straight line joining the object's origin to the shadow tip. The shading factor represents the percentage of cells shaded in the module and how this limits the irradiance available to that module. For instance, if no cells are shaded in the module, the shading factor is 1 and if all cells are shaded in a module then the shading factor becomes 0. The shading factor equation is given by

$$\text{sf} = 1 - (\text{shaded cells}/36). \quad (7)$$

The irradiance on each module is determined by multiplying the shading factor by the 1-min irradiance data obtained from the Australian Bureau of Meteorology [51]. This creates an authentic indication of the irradiance experienced by the modules when shading occurs in the environment. A clear day and variable day irradiance profiles are considered in the simulations. These irradiance profiles are shown in Figs. 2 and 3, respectively.

The P&O, PSO, and SA methods are all applied on the eight series-connected modules simulation model to assess the performance in tracking to the GMPP. Two different selections of irradiance data are considered. In the first case, 58 test cases are considered from April 1, 2010 when the panels experienced shading (starting at 1:36 pm AEST) and the irradiance is variable. In the second case, 18 test cases are considered from October 11, 2010 (starting at 1:36 pm AEST) when the panels experienced shading and the irradiance varies very slowly.

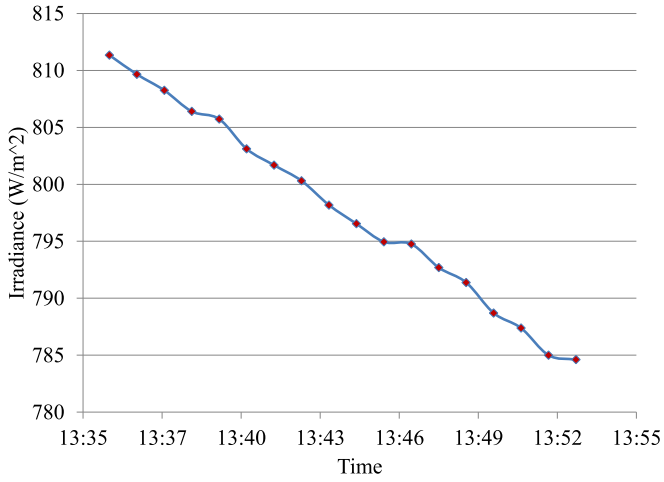

Fig. 2. Clear day irradiance profile.

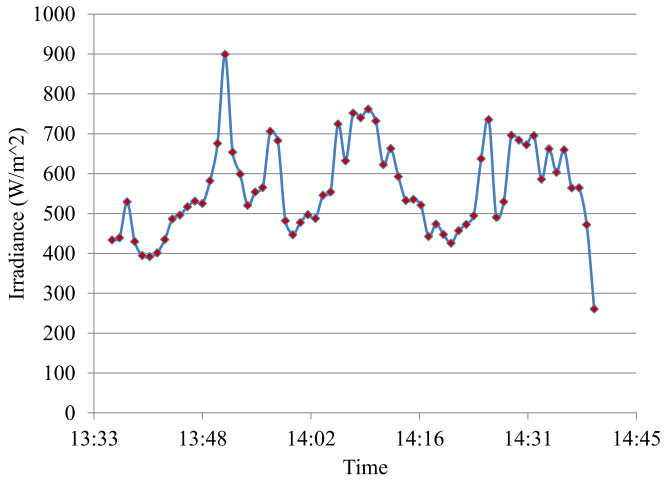

Fig. 3. Variable day irradiance profile.

Performance is recorded in terms of the time it takes the algorithm to track to near the MPP and the number of cases in which the algorithm converges to within 1%–5% of the GMPP location, the cases where it converges to a similar power level local MPP and when it does not converge.

The P&O method is implemented with a step size of 0.75 V and an initial voltage of 10 V. A perturbation is applied every 0.05 s. The PSO method is implemented with the following parameters $\omega = 0.4$, $c_1 = 1.2$, $c_2 = 1.6$ obtained from [52]. The method cycles through the particles and the current particle's voltage is applied every 0.05 s. The particles are kept within the range of 15–150 V. The SA algorithm is applied with an initial temperature of $25\,^{\circ}$C, final temperature $0.2\,^{\circ}$C, and temperature update constant of 0.8. Temperature update occurs every 0.4 s. These parameters are fairly arbitrarily selected based on observations of the technique with various parameter values, and show that a satisfactory performance of the technique can be achieved with limited optimization. The voltage was perturbed within the range of 14–144 V. The sampling time used was 0.2 s. During this sampling time, at $t = 0$ s, the algorithm is applied, at $t = 0.05$ s, the algorithm compares the current operating point with the previous best operating point, and then, decides whether to accept the new operating point. The remaining 0.15 s of the sample time enables the technique to return to the reference voltage (newly accepted or otherwise). This means that under changing irradiance, the technique should be able to detect that the power at its reference operating point is changing to enable more successful tracking.

VI. Results and Discussion

Figs. 4 and 5 demonstrate the voltage and power tracking of the P&O, PSO, and SA techniques, respectively, for one sample case. In this sample case, a single obstacle is placed in the environment, and leads to two MPPs being exhibited in the *P–V* characteristics as shown in Fig. 6. These MPPs have similar power, and the GMPP is only 11 W larger than the local MPP. Clearly in this case, it can be seen that while the P&O and PSO techniques do converge to within 5% of the known GMPP power, there is a voltage difference of about 17 V in the final operating point indicating that the technique has converged to a local MPP with similar power to the GMPP.

Several measures for the performance of each technique are considered for this implementation. First, the time taken by the algorithm to converge is given for the variable day irradiance profile in Table I, and for the clear day irradiance profile in Table II. For the SA algorithm, this time to converge refers to the time taken by the algorithm to track to near the final operating point without accepting any future operating points which are at a considerably lower power and far from the final operating point. For the P&O method, the convergence time is the time taken to arrive at a MPP and start oscillating around that point, and for the PSO technique, it is the time taken for all particles to converge to within 0.02 V of each other.

The convergence of each MPP technique is considered in Figs. 7 and 8 for the clear and variable day irradiance profiles, respectively. Various convergence measures are considered including a 1% to 5% convergence rating, and cases where the technique clearly converges to a local MPP that has a similar power to the GMPP. The 1% convergence rating gives a measure of the number of cases where the operating point converges to within 1% of the known voltage and 1% of the known power at the GMPP. The other measures are defined on the same basis. In each case, the convergence is expressed as a percentage of the 58 variable and 18 clear irradiance test cases that meet that requirement. The operating point is considered to have not converged if it has an error of more than 5% in the power when compared to the expected GMPP power. For the variable day irradiance profile, the P&O method converged to a local MPP with power similar to the GMPP in 6.9% of cases, the PSO method in 12.1% of cases, and the SA method in 8.6% of the tested cases. The P&O method did not converge in 43.1% of the cases, the PSO method in 20.7% of the cases, and the SA method in 12.1% of cases. For the clear day irradiance profile, the P&O method converged to a local MPP with power similar to the GMPP in 5.9% of the cases, the PSO method in 11.8% of the cases, and the SA method in 5.9% of the tested cases. The P&O method did not converge in 35.3% of the cases, the PSO method in 11.8% of the cases, and the SA method in 0.0% of the cases.

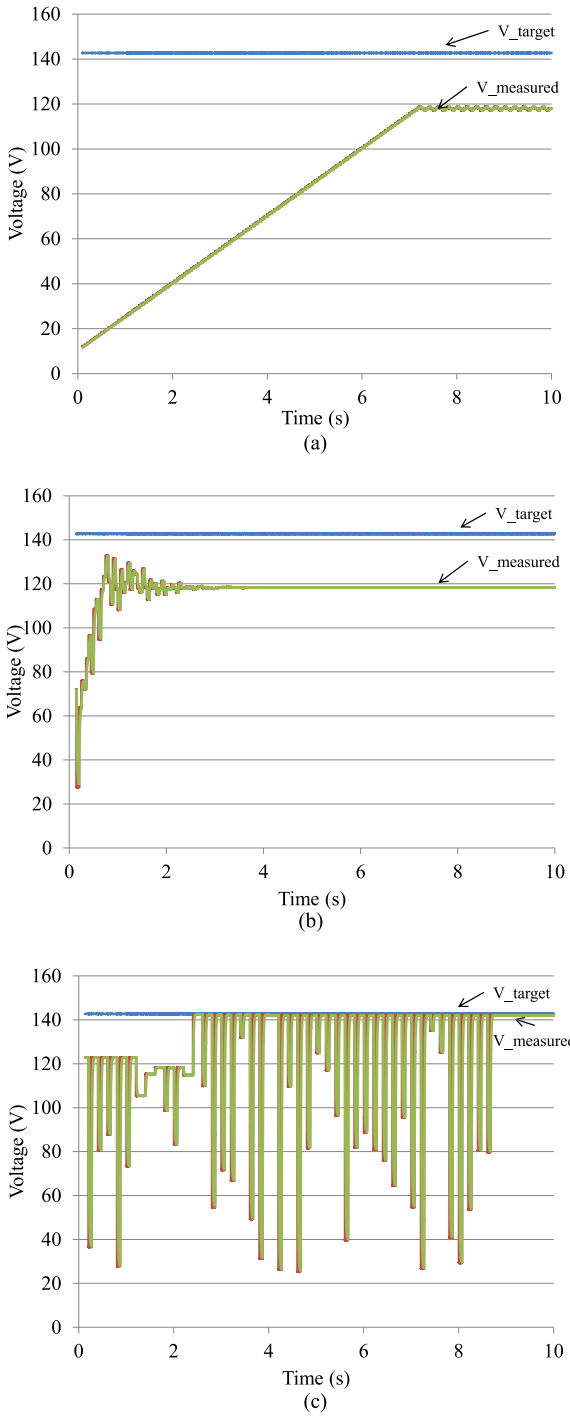

Fig. 4. Voltage–time chart of the sample case for MPPT implementations: (a) P&O, (b) PSO, and (c) SA.

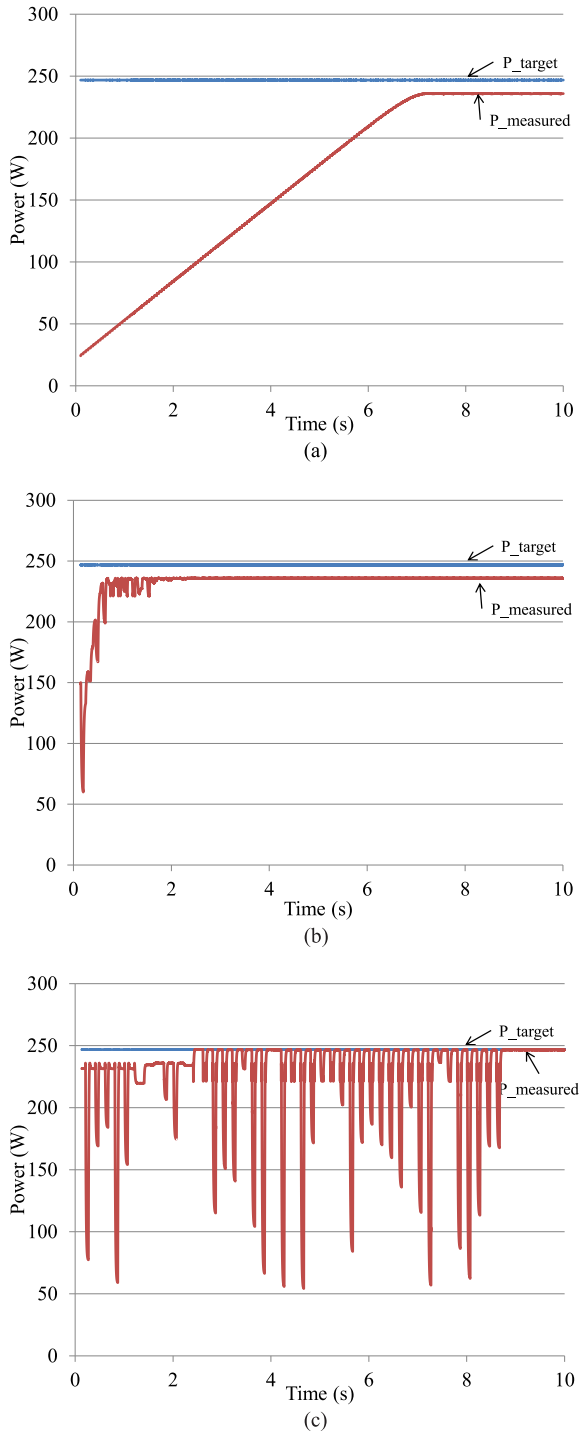

Fig. 5. Power–time chart of the sample case for MPPT implementations: (a) P&O, (b) PSO, and (c) SA.

The results show that the SA algorithm performs best in terms of the average, minimum, and maximum time to the vicinity of the MPP when compared with the other techniques for the variable day irradiance profile. In particular, the PSO technique for the variable day irradiance profile in a few test cases did not converge to any operating point, which is why the maximum in those cases is 10 s. For the clear day irradiance profile, the PSO technique exhibited a better time to find the MPP, showing that the performance of this technique is very dependent on the environmental conditions and the starting value.

These results show that when the 1% convergence criterion is applied, the performance of the PSO technique is superior to the other techniques. However, as the criterion is relaxed to a 5% convergence, the performance of the SA algorithm becomes considerably better than that of the P&O and PSO techniques. This is in line with the goals of the SA technique implementation

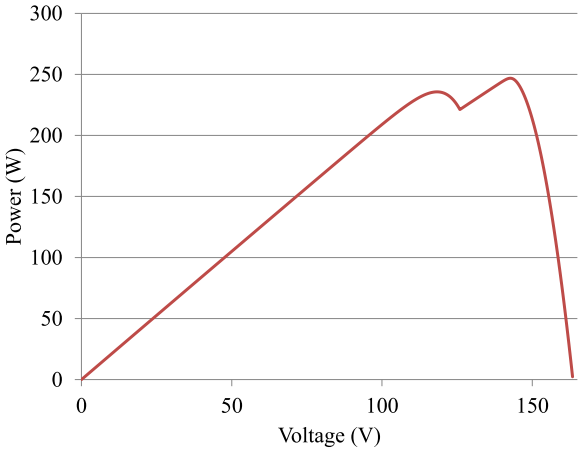

Fig. 6. *P– V* characteristics for the sample P&O, PSO, and SA voltage and power tracking.

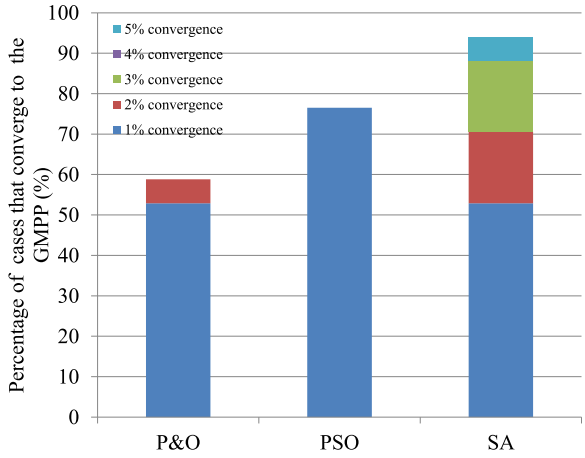

Fig. 7. Performance in converging to the GMPP—Clear day irradiance profile.

TABLE I
TIME TO MPP—VARIABLE DAY IRRADIANCE PROFILE

	P&O	PSO	SA
Average (s)	6.0	3.6	2.9
Standard Deviation (s)	0.9	1.8	1.6
Minimum (s)	4.8	7.0	0.2
Maximum (s)	8.3	10.0	7.4

TABLE II
TIME TO MPP—CLEAR DAY IRRADIANCE PROFILE

	P&O	PSO	SA
Average (s)	7.24	1.64	2.5
Standard Deviation (s)	0.76	0.51	1.73
Minimum (s)	5.85	0.65	0.2
Maximum (s)	8.35	2.6	7.0

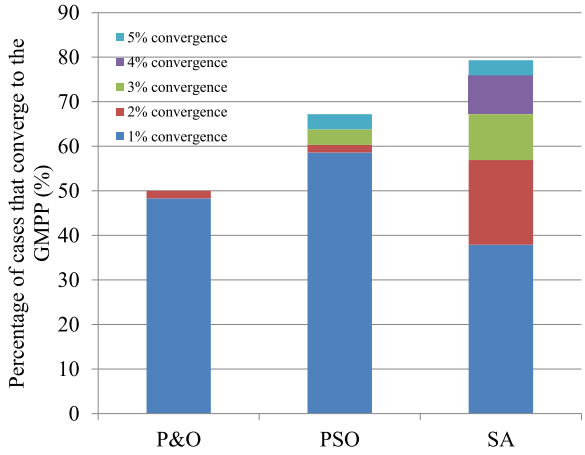

Fig. 8. Performance in converging to the GMPP—Variable day irradiance profile.

considered which is to converge to near the GMPP such that a local searching process could be initiated to perform fine tracking to the GMPP, similar to the approach suggested in [28] incorporating the PSO method for global searching and hill climbing for fine searching. The percentage of cases where the SA algorithm does not converge is far fewer than the percentage of cases where the PSO and P&O techniques do not converge. In fact, for the clear day irradiance profile, the SA method converges either to the GMPP or a MPP with similar power (within 5% of the GMPP power) for all test cases. The performance of the PSO technique may be improved by applying the approach described in [19] to select 60%–70% of the initial particle positions with consideration of the anticipated shadow. Taking these steps to improve the performance of the technique would add to the implementation complexity and reduce the universal applicability of the technique as some knowledge of the environment would be required to appropriately define the anticipated shading. The advantage of the SA technique, in this case, is that it can be applied with a truly random starting point and still converge in the majority of cases. The SA algorithm exhibits better performance with respect to converging to the GMPP when compared to the PSO and P&O methods as outlined above. As the SA algorithm has a complexity similar to that of the P&O technique and has fewer variables that need to be retained in memory than the PSO technique, it is a simple yet robust approach to achieving GMPPT under PSC.

The SA and PSO approaches are time-invariant optimization techniques to locate a global maxima, and as such, are unable to provide continuous tracking of the MPP. These techniques require a reinitialization condition to be applied to restart the searching when a change in the environmental conditions occurs. To assess the energy capture from the P&O, PSO, and SA methods under the same environmental conditions, the operation of the methods with a reset condition has been explored with the same obstacle placement and the already described variable and clear day irradiance profiles. The reset condition applied is given in (8) [27], where $P_{pv,\text{new}}$ is the most recent power measurement at the operating point, $P_{pv,\text{last}}$ is the previous power measurement at the operating point, and ΔP is some threshold

$$\frac{|P_{pv,\text{new}} - P_{pv,\text{last}}|}{P_{pv,\text{last}}} >= \Delta P. \tag{8}$$

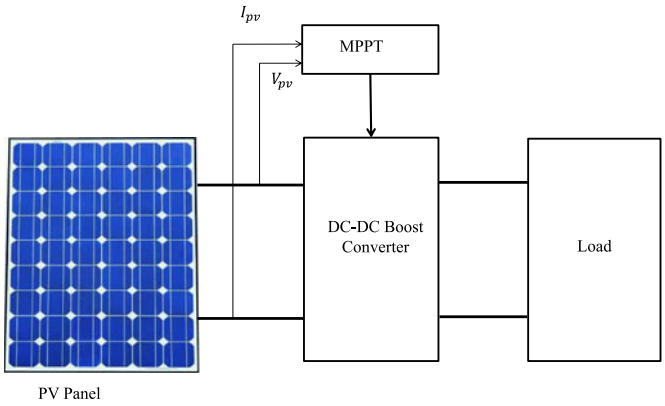

Fig. 9. Block diagram of the experimental setup.

The energy captured by each method under the clear and variable irradiance profiles considered shows the good performance of the PSO and SA methods under PSC. For the clear irradiance profile, the SA method captured 96.14% of the available energy, the PSO method captured 96.93% of the available energy, and the P&O method captured only 95.2% of the available energy. With the variable irradiance profile, the SA method captured 92.17% of the available energy, the PSO method captured 95.23% of the available energy, and the P&O method captured only 71.98% of the available energy. Under these simulation conditions, the PSO method has performed slightly better than the SA method, most likely due to the fact that, if implemented effectively, it takes less time to search than the current, not fully optimized, implementation of the SA method.

VII. Experimental Validation

Experimental validation is shown in this paper by performing several tests of the SA algorithm to confirm that it has good performance in converging to the GMPP. Additionally, in this section for comparison, the PSO and P&O methods are implemented using the same experimental setup.

The block diagram of the experimental implementation is shown in Fig. 9. The BP380 PV modules are connected to a dc–dc converter, via a Textronix AC662 current probe, and then connected to the load. Analog current and voltage measurements are fed into the Labview program via a NI USB-6008 data acquisition device, where the control algorithm is implemented. Labview is utilized as it provides an effective method for the MPPT algorithm to be easily modified during testing to improve performance and allows the SA algorithm to be implemented as embedded MATLAB scripts. The duty cycle, input power, voltage, and current to the converter are all monitored on the Labview interface as shown in Fig. 10. Experimental tests are implemented with initial temperature 20 °C, final temperature 0.2 °C, and cooling rate 0.55, and with the temperature update occurring every three iterations. The Labview program performs the control algorithm, and writes an analog output between 0 and 5 V to a PIC microcontroller, which then outputs the PWM signal to control the MOSFETs. PSC were established by covering one panel with layers of fabric, similar to the approach in [53]. Sixty-four different test cases are considered, where the irradiance may be uniform or nonuniform, with either one or two layers

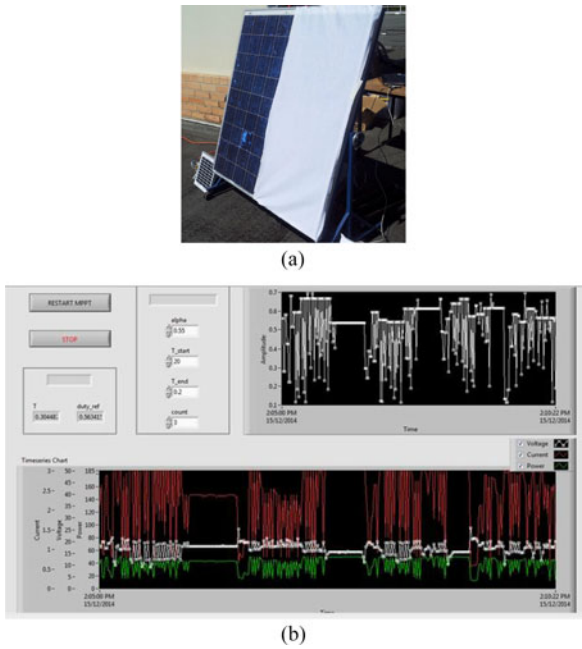

Fig. 10. Experimental setup and Labview interface for MPPT implementation. (a) Experimental setup. (b) Labview interface (SA tracking).

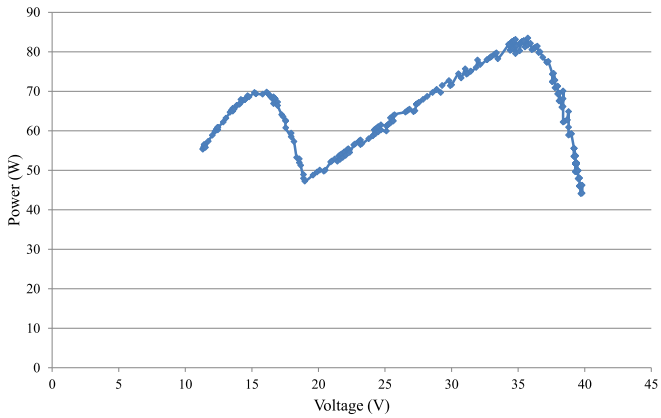

Fig. 11. Sample *P–V* characteristics for experimental testing.

of fabric. In 79% of the test cases, the SA algorithm converged to the GMPP, and in 4.69%, it converged to a MPP with very similar power to the GMPP. For 14% of the test cases, the method either did not converge to the GMPP or converged to a MPP with considerably less power.

The SA, PSO, and P&O methods are all applied as MPPT methods in the Labview interface to compare their performance in converging to the GMPP. In each case, a *P–V* curve trace is completed before the test to indicate where the MPPs will most likely be located. In these comparison tests, one of the two panels is covered with a layer of white fabric, and each algorithm is performed six to eight times from the initialization condition to determine how well each method will track the GMPP. A sample *P–V* curve showing the approximate characteristics is shown in Fig. 11. As testing was performed in the outdoor uncontrolled environment, there was significant variation in the environmental conditions during each test, which in some cases lead to the

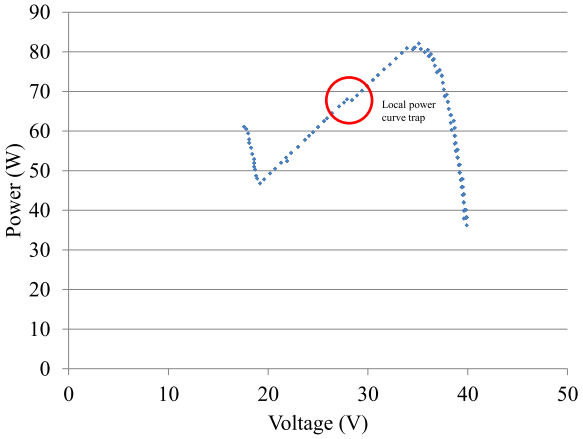

Fig. 12. *P–V* characteristic for P&O experimental implementation sample case.

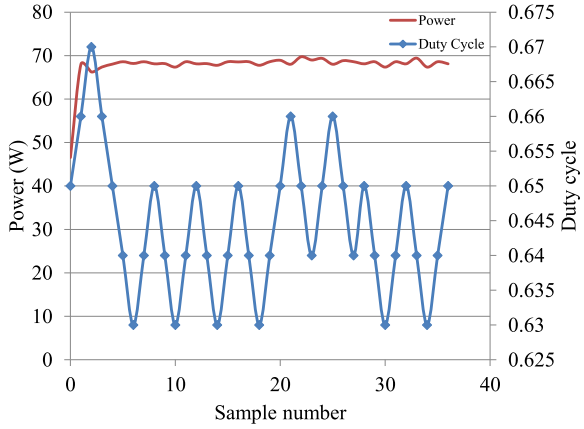

Fig. 13. Sample tracking using P&O for *P–V* characteristic shown in Fig. 12.

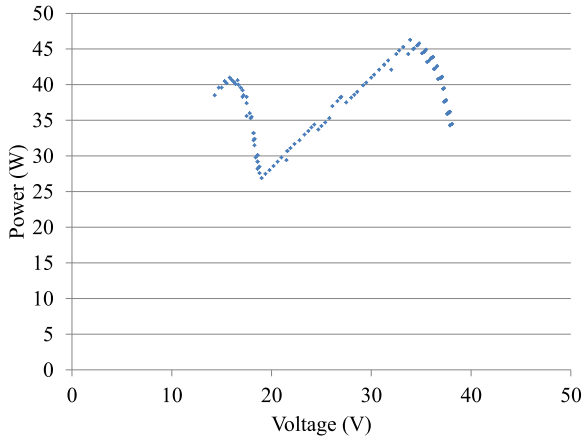

Fig. 14. *P– V* characteristic for PSO experimental implementation sample case.

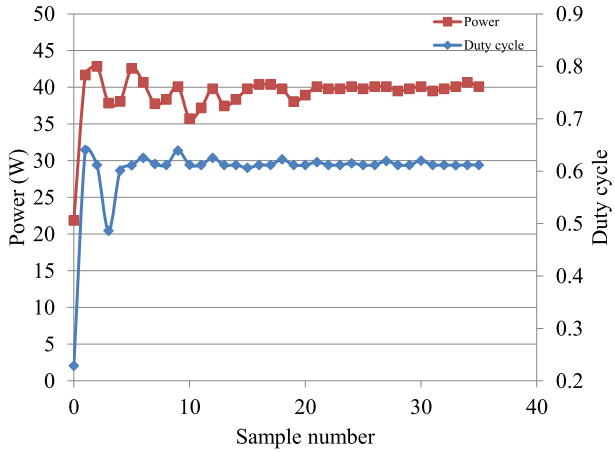

Fig. 15. Sample tracking using PSO for *P–V* characteristic shown in Fig. 14.

PSO and P&O algorithms either searching in the wrong direction or taking a considerable amount of time to search the solution space. Of the seven tests for the SA method, five converged to the GMPP and two converged to local MPPs. When the PSO method was applied, five of the eight test cases converged to the GMPP. The speed in converging to the GMPP using the PSO method varied greatly in the different tests. In the best case, the PSO method found the GMPP after only ten samples, but in the worst case 368 samples were required due to the changing environmental conditions. The P&O method converged in three of the six test cases considered. In some of the test cases, it became clear that the P&O method had become trapped in a local power trap [54] as the method continued to oscillate around a point far from any MPP. There were also several cases where the method started to track in the wrong direction as the environmental conditions changed. In one cases, this required 220 samples for the P&O method to finally track to and start oscillating around the actual MPP location. Another key observation from the P&O experimental tests highlights that the ability of the technique to converge to the GMPP was very dependent on the initial duty cycle selected in the implementation. In all the cases where the method converged to the local MPP, the initial duty cycle had set the technique up to achieve this by being more closely located to the local MPP than to the global MPP.

Sample experimental tracking cases for each method are now described. The *P–V* characteristics experienced for the sample P&O tracking are shown in Fig. 12. From inspection of this figure, there is a small power curve trap [54] located at about 28 V. The tracking case shown in Fig. 13 demonstrates the tracking of the P&O method under these environmental conditions, with a starting duty cycle of 0.65. It is clear from these results that the method has become trapped in the local power trap, which means that it has not successfully located the global maxima. *P–V* characteristics for the sample experimental PSO tracking are shown in Fig. 14. It can be seen that the curve trace is not completely smooth, but this is unavoidable due to the changing environmental conditions. A sample PSO tracking under these environmental conditions is shown in Fig. 15. The PSO method converges quickly, however, it converges to the local peak power. *P–V* characteristics for the sample SA tracking case are shown in Fig. 16. This clearly shows that the GMPP is about 80 W. The tracking of the SA method under these conditions is shown in Fig. 17. Despite the fact that the SA method requires a larger number of samples than shown with the P&O and PSO methods, it can successfully track to the GMPP. The characteristics that each method is tested under are not

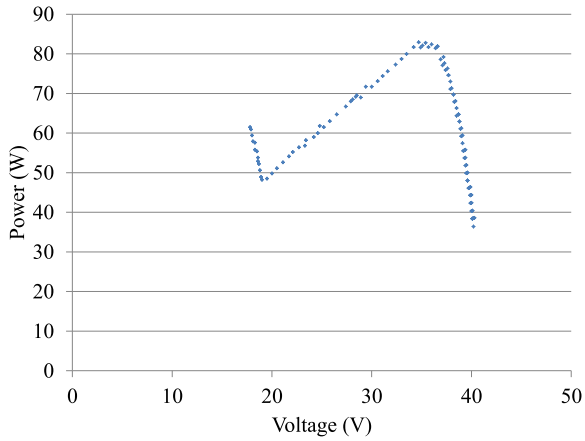

Fig. 16. *P–V* characteristic for SA experimental implementation sample case.

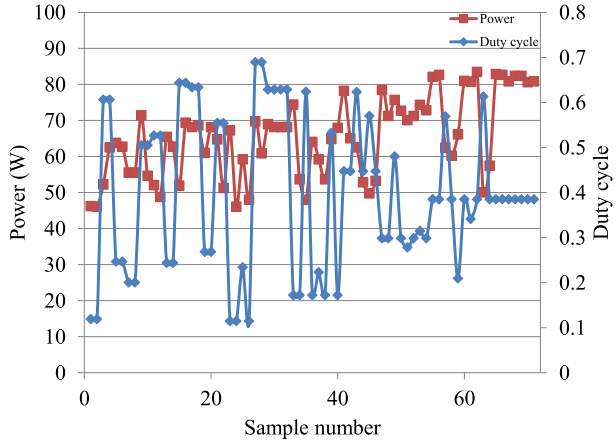

Fig. 17. Sample tracking using SA for *P–V* characteristic shown in Fig. 16.

identical as the experiment is performed in the outdoor environment. Each characteristic, however, exhibits a local peak at about 17 V and a global peak at about 35 V.

VIII. Key Parameters of the SA Method and Their Effects on the Performance

The SA implementations considered in the simulation studies and experimental validation presented in this paper rely on fairly arbitrarily selected parameters for the method. This does lead to some disadvantages in the operation of the technique, primarily in the large search range that samples may come from, the potentially large number of samples required to converge, and the fact that the method will continue to sample even after the best operating point has been located. Extensive studies of the key parameters have been completed to assess how each parameter will effect both the ability of the method to converge and the number of samples required. These key parameters include initial temperature, cooling rate, cooling frequency, acceptance probability threshold, neighbourhood size, stopping temperature, stopping criterion, and cooling function. Due to space restrictions, only those parameters which have been shown to have a significant effect will be considered in this section. In each case, the SA method with the modified parameters is applied 100 times on 30 different *P–V* characteristics.

A. Linear Neighbourhood Size Reduction Function

The neighbourhood range is reduced linearly after each temperature update occurs according to the relationship

$$\text{size} = -5.5 \times \text{update} + 135.5 \tag{9}$$

where size is the size of the neighbourhood and update represents the number of temperature updates that have occurred.

Reducing the neighbourhood size will not influence the number of samples required by the SA algorithm to converge. With a linear neighbourhood reduction function, the percentage of tested cases that converge is 93.7%. The advantage of reducing the neighbourhood size is that it restricts the voltage range that the method can sample within which should reduce the oscillations observed when sampling.

B. Stopping Criterion

A stopping criterion has been implemented where the SA algorithm is stopped if the solution quality has not improved for a particular number of samples. Stopping criterion constants between two and ten samples with no improvement are considered. As the stopping criterion constant is increased, the number of samples required is increased and the performance improves. With an average of 55 samples, the method will converge in 70% of the cases. The stopping criterion has a significant effect on reducing the number of samples required, however it does not significantly improve the performance.

C. Lundy Cooling Schedule

The Lundy cooling schedule is given by (10), where T_k is the new temperature, T_{k-1} is the previous temperature, and β is some constant

$$T_k = \frac{T_{k-1}}{1 + \beta T_{k-1}}. \tag{10}$$

As the Lundy cooling constant β is decreased, the number of samples required and the number of cases that converge to the GMPP increase. With 100 samples, the Lundy cooling function leads to an average convergence of 98%. The variation in the number of samples required and the average convergence for the Lundy method with different cooling constants is shown in Fig. 18.

D. Simulated Quenching (SQ)

SQ is proposed as a way to achieve GMPPT quicker than with other cooling schedules. The SQ cooling function is given in (11), where C is a constant, the initial temperature (T_0) is 25 °C, and k represents the number of samples

$$T_k = \frac{T_0}{\exp{(1 - C)k}}. \tag{11}$$

SQ shows good performance with, on average, over 80% of cases converging with only 40 samples. The variation of the average number of samples and average percentage of cases that converge is shown in Fig. 19.

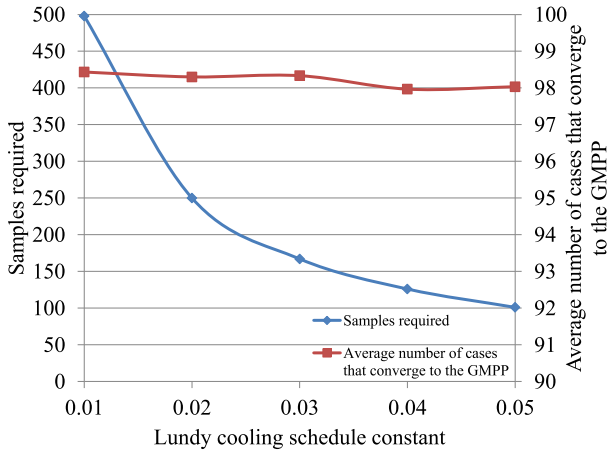

Fig. 18. Samples required and average convergence to the GMPP with increasing Lundy cooling constant.

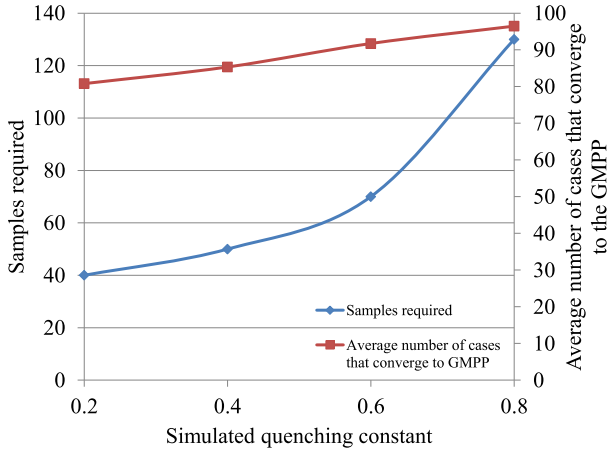

Fig. 19. Samples required and average convergence to the GMPP with increasing SQ cooling constant.

E. Summary

The four cases detailed above show that some parameter variations can be used to improve the performance of the SA method. No single parameter variation in isolation, however, is able to achieve the goals of fewer samples and better convergence simultaneously. Future research will include combining the effects of multiple parameter variations with a local searching methodology to enable accurate GMPPT to occur with minimal samples.

IX. Conclusion

A SA-based MPPT technique has been proposed for achieving GMPPT for PV systems experiencing nonuniform environmental conditions. The performance of the technique in tracking to the GMPP for real-irradiance data with a simulated shadow path is compared to the performance of the P&O and PSO methods in tracking under the same irradiance conditions. Results show the improved performance of the proposed technique in converging to the GMPP. The algorithm achieves GMPP or near GMPP with only a slight increase in computational complexity when compared to the P&O technique and requires fewer parameters to be stored in memory from one iteration to the next than the PSO technique. The ability of the proposed SA technique to track to the GMPP is not limited by the starting value used in the algorithm. Experimental results demonstrate a practical application of the method, and parameter studies suggest future enhancements to improve the convergence speed and accuracy.

References

[1] S. Lyden, M. E. Haque, A. Gargoom, and M. Negnevitsky, "Review of maximum power point tracking approaches suitable for PV systems under partial shading conditions," in *Proc. Austr. Univ. Power Eng. Conf.*, 2013, pp. 1–6.

[2] W. Xiao, A. Elnosh, V. Khadkikar, and H. Zeineldin, "Overview of maximum power point tracking technologies for photovoltaic power systems," in *Proc. IEEE Ind. Electron. Soc. Conf.*, 2011, pp. 3900–3905.

[3] B. Subudhi and R. Pradhan. (2013, Jan.). A comparative study on maximum power point tracking techniques for photovoltaic power systems. *IEEE Trans. Sustainable Energy*. [Online]. *4(1)*, pp. 89–98. Available: http://ieeexplore.ieee.org/lpdocs/epic03/wrapper.htm?arnumber=6249779

[4] T. Esram and P. L. Chapman, "Comparison of photovoltaic array maximum power point tracking techniques," *IEEE Trans. Energy Convers.*, vol. 22, no. 2, pp. 439–449, Jun. 2007.

[5] M. A. G. de Brito, L. Galotto, L. P. Sampaio, G. de Azevedo e Melo, and C. A. Canesin, "Evaluation of the main MPPT techniques for photovoltaic applications," *IEEE Trans. Ind. Electron.*, vol. 60, no. 3, pp. 1156–1167, Mar. 2013.

[6] A. Bidram, A. Davoudi, and R. S. Balog, "Control and circuit techniques to mitigate partial shading effects in photovoltaic arrays," *IEEE J. Photovoltaics*, vol. 2, no. 4, pp. 532–546, Oct. 2012.

[7] H. Patel and V. Agarwal, "MATLAB-based modeling to study the effects of partial shading on PV array characteristics," *IEEE Trans. Energy Convers.*, vol. 23, no. 1, pp. 302–310, Mar. 2008.

[8] P. Bakas, A. Marinopoulos, and B. Stridh. (2012, Jun.). Impact of PV module mismatch on the PV array energy yield and comparison of module, string and central MPPT. in *Proc. IEEE Photovolt. Spec. Conf.* [Online]. pp. 001393–001398. Available: http://ieeexplore.ieee.org/lpdocs/epic03/wrapper.htm?arnumber=6317859

[9] G. Escobar, C. N. M. Ho, and S. Pettersson, "Maximum power point searching method for partial shaded PV strings," in *Proc. IEEE Ind. Electron. Soc. Conf.*, 2012, pp. 5726–5731.

[10] H. Patel and V. Agarwal, "Maximum power point tracking scheme for PV systems operating under partially shaded conditions," *IEEE Trans. Ind. Electron.*, vol. 55, no. 4, pp. 1689–1698, Apr. 2008.

[11] N. Femia, G. Lisi, G. Petrone, G. Spagnuolo, and M. Vitelli, "Distributed maximum power point tracking of photovoltaic arrays: Novel approach and system analysis," *IEEE Trans. Ind. Electron.*, vol. 55, no. 7, pp. 2610–2621, Jul. 2008.

[12] S. Poshtkouhi, V. Palaniappan, M. Fard, and O. Trescases, "A general approach for quantifying the benefit of distributed power electronics for fine grained MPPT in photovoltaic applications using 3D modeling," *IEEE Trans. Power Electron.*, vol. 27, no. 11, pp. 4656–4666, Nov. 2012.

[13] R. Alonso, E. Roman, A. Sanz, V. E. M. Santos, and P. Ibanez, "Analysis of inverter-voltage influence on distributed MPPT architecture performance," *IEEE Trans. Ind. Electron.*, vol. 59, no. 10, pp. 3900–3907, Oct. 2012.

[14] L. Zhou, Y. Chen, K. Guo, and F. Jia, "New approach for MPPT control of photovoltaic system with mutative scale dual-carrier chaotic search," *IEEE Trans. Power Electron.*, vol. 26, no. 4, pp. 1038–1048, Apr. 2011.

[15] P. Lei, Y. Li, and J. Seem, "Sequential ESC based global MPPT control for photovoltaic array with variable shading," *IEEE Trans. Sustainable Energy*, vol. 2, no. 3, pp. 348–358, Jul. 2011.

[16] E. Koutroulis and F. Blaabjerg, "A new technique for tracking the global maximum power point of PV arrays operating under partial-shading conditions," *IEEE J. Photovoltaics*, vol. 2, no. 2, pp. 184–190, Apr. 2012.

[17] B. Alajmi, K. Ahmed, S. Finney, and B. Williams, "Fuzzy logic controlled approach of a modified hill climbing method for maximum power point in microgrid stand-alone photovoltaic system," *IEEE Trans. Power Electron.*, vol. 26, no. 4, pp. 1022–1030, Apr. 2011.

[18] M. Miyatake, T. Inada, I. Hiratsuka, Z. Hongyan, H. Otsuka, and M. Nakano, "Control characteristics of a fibonacci-search-based maximum power point tracker when a photovoltaic array is partially shaded," in *Proc. Int. Power Electron. Motion Control Conf.*, 2004, vol. 2, pp. 816–821.
[19] M. Miyatake, M. Veerachary, F. Toriumi, N. Fujii, and H. Ko, "Maximum power point tracking of multiple photovoltaic arrays: A PSO approach," *IEEE Trans. Aerosp. Electron. Syst.*, vol. 47, no. 1, pp. 367–380, Jan. 2011.
[20] R. Ramaprabha, B. Mathur, A. Ravi, and S. Aventhika, "Modified fibonacci search based MPPT scheme for SPVA under partial shaded conditions," in *Proc. Int. Conf. Emerg. Trends Eng. Technol*, 2010, pp. 379–384.
[21] A. Pandey, N. Dasgupta, and A. Mukerjee, "High-performance algorithms for drift avoidance and fast tracking in solar MPPT system," *IEEE Trans. Energy Convers.*, vol. 23, no. 2, pp. 681–689, Jun. 2008.
[22] D. Sera, R. Teodorescu, J. Hantschel, and M. Knoll, "Optimized maximum power point tracker for fast-changing environmental conditions," *IEEE Trans. Ind. Electron.*, vol. 55, no. 7, pp. 2629–2637, Jul. 2008.
[23] A. K. Abdelsalam, A. M. Massoud, S. Ahmed, and P. N. Enjeti, "High-performance adaptive perturb and observe MPPT technique for photovoltaic-based microgrids," *IEEE Trans. Power Electron.*, vol. 26, no. 4, pp. 1010–1021, Apr. 2011.
[24] W.-S. Jwo, C.-C. Tong, and C.-J. Chao. (2010, Jun.). Firmware implementation of an adaptive solar cell maximum power point tracking based on PSoC. in *Proc. IEEE Photovoltaic Spec. Conf*. [Online]. pp. 000407–000411. Available: http://ieeexplore.ieee.org/lpdocs/epic03/wrapper.htm?arnumber=5616803
[25] K. Ishaque, Z. Salam, S. Mekhilef, and A. Shamsudin, "Parameter extraction of solar photovoltaic modules using penalty-based differential evolution," *Appl. Energy*, vol. 99, pp. 297–308, 2012.
[26] L. R. Chen, C. H. Tsai, Y. L. Lin, and Y. S. Lai, "A biological swarm chasing algorithm for tracking the PV maximum power point," *IEEE Trans. Energy Convers.*, vol. 25, no. 2, pp. 484–493, Jun. 2010.
[27] L. Yi-Hwa, H. Shyh-Ching, H. Jia-Wei, and L. Wen-Cheng, "A particle swarm optimization-based maximum power point tracking algorithm for PV systems operating under partially shaded conditions," *IEEE Trans. Energy Convers.*, vol. 27, no. 4, pp. 1027–1035, Dec. 2012.
[28] K. Ishaque and Z. Salam, "A deterministic particle swarm optimization maximum power point tracker for photovoltaic system under partial shading condition," *IEEE Trans. Ind. Electron.*, vol. 60, no. 8, pp. 3195–3206, Aug. 2013.
[29] S. Kirkpatrick, D. J. Gelatt, and M. P. Vecchi, "Optimization by simulated annealing," *Science*, vol. 220, no. 4598, pp. 671–680, 1983.
[30] V. Černý, "Thermodynamical approach to the traveling salesman problem: An efficient simulation algorithm," *J. Optim. Theory Appl.*, vol. 45, no. 1, pp. 41–51, Jan. 1985.
[31] S.-I. Ao and L. Gelman, *Electrical Engineering and Intelligent Systems*. Dordrecht, The Netherlands: Springer, 2012.
[32] Y. A. Katsigiannis, P. S. Georgilakis, and E. S. Karapidakis, "Hybrid simulated annealing tabu search method for optimal sizing of autonomous power systems with renewables," *IEEE Trans. Sustainable Energy*, vol. 3, no. 3, pp. 330–338, Jul. 2012.
[33] Y.-M. Chen, C.-H. Lee, and H.-C. Wu, "Calculation of the optimum installation angle for fixed solar-cell panels based on the genetic algorithm and the simulated-annealing method," *IEEE Trans. Energy Convers.*, vol. 20, no. 2, pp. 467–473, Jun. 2005.
[34] J. Mitra, "Application of computational intelligence in optimal expansion of distribution systems," in *Proc. IEEE Power and Energy Soc. Gen. Meet.*, Jul. 2008, pp. 1–8.
[35] Y. Yang, W. Pei, and Z. Qi, "Optimal sizing of renewable energy and CHP hybrid energy microgrid system," in *Proc. IEEE PES Innov. Smart Grid Technol.*, May 2012, pp. 1–5.
[36] T. Sutthibun and P. Bhasaputra, "Multi-objective optimal distributed generation placement using simulated annealing," in *Proc. Int. Conf. Electr. Eng./Electron. Comput. Telecommun. Inf. Technol.*, 2010, pp. 810–813.
[37] A. K. Barnes, J. C. Balda, A. Escobar-Mejia, and S. O. Geurin, "Placement of energy storage coordinated with smart PV inverters," in *Proc. IEEE PES Innov. Smart Grid Technol.*, Jan. 2012, pp. 1–7.
[38] V. Evangelin Jeba, S. Ravichandran, and R. Kumudini Devi, "Optimal control of grid connected variable speed wind energy conversion system," in *Proc. Int. Conf. Energy Efficient Technol. Sustainability*, Apr. 2013, pp. 393–399.
[39] D. L. Anton, S. L. Garrison, M. Gorensek, S. R. Sherman, R. Carapellucci, and L. Giordano, "Modeling and optimization of an energy generation island based on renewable technologies and hydrogen storage systems," *Int. J. Hydrogen Energy*, vol. 37, no. 3, pp. 2081–2093, 2012.
[40] M. A. Azam, S. Abdullah-Al-Nahid, M. A. Kabir, and S. M. H. Chowdhury, "Microcontroller based maximum power tracking of PV using stimulated annealing algorithm," in *Proc. Int. Conf. Informat. Electron. Vis.*, May 2012, pp. 298–303.
[41] S. A.-H. Soliman and A.-A. H. Mantawy, *Modern Optimization Techniques With Applications in Electric Power Systems*. Dordrecht, The Netherlands: Springer, 2011.
[42] B. McCallum, "Blind deconvolution by simulated annealing," *Opt. Commun.*, vol. 75, no. 2, pp. 101–105, 1990.
[43] J. Ohtsubo and K. Nakajima, "Image recovery by simulated annealing with known Fourier modulus," *Opt. Commun.*, vol. 86, no. 3, pp. 265–270, 1991.
[44] K. Wong and C. Fung, "Simulated annealing based economic dispatch algorithm," *IEE Proc., Gener., Transmiss. Distrib.*, vol. 140, no. 6, pp. 509–515, 1993.
[45] M. A. Elgendy, B. Zahawi, and D. J. Atkinson, "Assessment of perturb and observe MPPT algorithm implementation techniques for PV pumping applications," *IEEE Trans. Sustainable Energy*, vol. 3, no. 1, pp. 21–33, Jan. 2012.
[46] G. Zäpfel, R. Braune, and M. Bögl, *Metaheuristic Search Concepts: A Tutorial With Applications to Production and Logistics*. Dordrecht, The Netherlands: Springer, 2010.
[47] D. L. Poole and A. K. Mackworth, *Artificial Intelligence: Foundations of Computational Agents*. Cambridge, U.K.: Cambridge Univ. Press, 2010.
[48] A. Chatterjee, A. Keyhani, and D. Kapoor, " Identification of photovoltaic source models," *IEEE Trans. Energy Convers.*, vol. 26, no. 3, pp. 883–889, Sep. 2011.
[49] M. G. Villalva, J. R. Gazoli, and E. R. Filho, "Comprehensive approach to modeling and simulation of photovoltaic arrays," *IEEE Trans. Power Electron.*, vol. 24, no. 5, pp. 1198–1208, 2009.
[50] BP 380 80 W photovoltaic module datasheet. [Online]. Available: http://www.solarcharge.com.au/docs/off-grid-solar-panel-BP-80-Watt.pdf
[51] Bureau of Meteoroloy. (2012). One Minute Solar Data. [Online]. Available: http://www.bom.gov.au/climate/data/oneminsolar/about-IDCJAC0022.shtml
[52] K. Ishaque, Z. Salam, M. Amjad, and S. Mekhilef, "An improved particle swarm optimization (PSO)-based MPPT for PV with reduced steady state oscillation," *IEEE Trans. Power Electron.*, vol. 27, no. 8, pp. 3627–3638, Aug. 2012.
[53] S. Moballegh and J. Jiang, "Modeling, prediction, and experimental validations of power peaks of PV arrays under partial shading conditions," *IEEE Trans. Sustainable Energy*, vol. 5, no. 1, pp. 293–300, Jan. 2014.
[54] D. C. Jones and R. W. Erickson, "Probabilistic analysis of a generalized perturb and observe algorithm featuring robust operation in the presence of power curve traps," *IEEE Trans. Power Electron.*, vol. 28, no. 6, pp. 2912–2926, Jun. 2013.

Sarah Lyden (S'12) received the Graduate degree with a B.Sc.-B.E.(Hons.) and the Ph.D. degree in engineering from the University of Tasmania, Hobart, Tas., Australia, in 2011 and 2015, respectively.

She is currently a Lecturer at the School of Engineering and ICT, University of Tasmania. Her research interests include control and grid integration of renewable energy sources, microgrid systems, and engineering education.

Md. Enamul Haque (M'97–SM'10) received the Graduate degree in electrical and electronic engineering from the Rajshahi University of Engineering Technology (formerly, the Bangladesh Institute of Technology), Rajshahi, Bangladesh, in 1995, the M.Eng. degree in electrical engineering from University Technology Malaysia, Kuala Lumpur, Malaysia, in 1998, and the Ph.D. degree in electrical engineering from the University of New South Wales, Sydney, N.S.W., Australia, in 2002.

He is currently a Senior Lecturer in renewable energy and power systems at the School of Engineering, Deakin University, Geelong, Vic., Australia. His research interests include smart energy systems, control and grid integration of renewable energy sources and energy storage systems, microgrid system with hybrid wind/solar/fuel cell systems, and power electronics applications in smart grid and renewable energy systems.